J. Fluid Mech. (1972), *vol.* 54, *part* 2, *pp.* 263–288
Printed in Great Britain

The mechanics of an organized wave in turbulent shear flow. Part 3. Theoretical models and comparisons with experiments

By W. C. REYNOLDS AND A. K. M. F. HUSSAIN†
Department of Mechanical Engineering, Stanford University

(Received 18 October 1971)

The dynamical equations governing small amplitude wave disturbances in turbulent shear flows are derived. These equations require additional equations or assumptions about the wave-induced fluctuations in the turbulence Reynolds stresses before a closed system can be obtained. Some simple closure models are proposed, and the results of calculations using these models are presented. When the predictions are compared with our data for channel flow, we find it essential that these oscillations in the Reynolds stresses be included in the model. A simple eddy-viscosity representation serves surprisingly well in this respect.

1. Recapitulation

In this paper we summarize the theoretical work associated with our experimental studies of organized waves in turbulent shear flows (Hussain & Reynolds 1972, hereafter referred to as II). Motivations for this work were elaborated previously (Hussain & Reynolds 1970*a*, hereafter referred to as I), and include interest in possible wave theories of turbulent shear flow (Landahl 1967). This work is described in more detail in our report Hussain & Reynolds (1970*b*), hereafter referred to as R.

The experiments reported in II deal with two-dimensional waves introduced by vibrating ribbons in a fully developed turbulent channel flow. The ribbon-induced streamwise velocity component $\tilde{u}_1$ was measured using a hot-wire anemometer and special signal-averaging techniques; these data form the basis for comparison with the models to be discussed here.

In both the theory and experiment we represent a fluctuating signal by

$$f = \bar{f} + \tilde{f} + f', \tag{1.1}$$

where $\bar{f}$ is the mean (time-averaged) contribution, $\tilde{f}$ is the periodic wave and f' corresponds to the turbulent motion. Straightforward time averaging determines $\bar{f}$. Then, the *phase average*, i.e. the average over a large ensemble of points having the same phase with respect to a reference oscillator (e.g. the vibrating ribbons), is (see I)

$$\langle f \rangle = \bar{f} + \tilde{f}. \tag{1.2}$$

† Present address: Department of Mechanical Engineering, University of Houston, Houston, Texas.

In effect, the phase-averaging process rejects the background turbulence and extracts only the organized motions from the total signal. Some useful properties that follow from the basic definitions of time and phase averages are

$$\left.\begin{array}{lll} \langle f' \rangle = 0, & \tilde{\bar{f}} = 0, & \overline{f'} = 0, \\ \overline{\tilde{f}\bar{g}} = \tilde{f}\bar{g}, & \langle \tilde{f}\bar{g} \rangle = \tilde{f}\langle g \rangle, & \langle \bar{f}\bar{g} \rangle = \bar{f}\langle g \rangle, \\ \overline{\langle f \rangle} = \bar{f}, & \langle \tilde{f} \rangle = \tilde{f}, & \overline{\tilde{f}g'} = \langle \tilde{f}g' \rangle = 0. \end{array}\right\} \tag{1.3}$$

The first relation states the random nature of the background turbulence and the last that the background turbulence and the organized periodic (wave) motion are uncorrelated. These relationships are invoked in the derivation of the dynamical equations for the organized wave.

2. Dynamical equations for the organized motion

We start with the Navier–Stokes equations in normalized form; the length scale is δ, the velocity scale is U_r and the Reynolds number is $U_r\delta/\nu$. For incompressible constant-property flow, the continuity and momentum equations may be written using the summation convention as

$$\partial u_i/\partial x_i = 0 \tag{2.1a}$$

and

$$\frac{\partial u_i}{\partial t} + u_j \frac{\partial u_i}{\partial x_j} = -\frac{\partial p}{\partial x_i} + \frac{1}{Re}\frac{\partial^2 u_i}{\partial x_j \partial x_j}. \tag{2.1b}$$

Following the decomposition outlined above, we write velocity and pressure fields as

$$u_i = \bar{u}_i + \tilde{u}_i + u_i', \tag{2.2a}$$

$$p = \bar{p} + \tilde{p} + p'. \tag{2.2b}$$

On substituting (2.2a) into (2.1a), time averaging and then phase averaging, the component continuity equations are found to be

$$\frac{\partial \bar{u}_i}{\partial x_i} = \frac{\partial \tilde{u}_i}{\partial x_i} = \frac{\partial u_i'}{\partial x_i} = 0. \tag{2.3a,b,c}$$

After substituting (2.2) into (2.1b) and phase averaging, one finds

$$\frac{\partial \tilde{u}_i}{\partial t} + \bar{u}_j \frac{\partial \bar{u}_i}{\partial x_j} + \bar{u}_j \frac{\partial \tilde{u}_i}{\partial x_j} + \tilde{u}_j \frac{\partial \bar{u}_i}{\partial x_j} + \frac{\partial}{\partial x_j}\langle u_i' u_j' \rangle + \frac{\partial}{\partial x_j}(\tilde{u}_i \tilde{u}_j)$$
$$= -\left(\frac{\partial \bar{p}}{\partial x_i} + \frac{\partial \tilde{p}}{\partial x_i}\right) + \frac{1}{Re}\left(\frac{\partial^2 \bar{u}_i}{\partial x_j \partial x_j} + \frac{\partial^2 \tilde{u}_i}{\partial x_j \partial x_j}\right). \tag{2.4}$$

The time average of (2.4) gives the equations for the mean field:

$$\bar{u}_j \frac{\partial \bar{u}_i}{\partial x_j} = -\frac{\partial \bar{p}}{\partial x_i} + \frac{1}{Re}\frac{\partial^2 \bar{u}_i}{\partial x_j \partial x_j} - \frac{\partial}{\partial x_j}(\overline{u_i' u_j'}) - \frac{\partial}{\partial x_j}(\overline{\tilde{u}_i \tilde{u}_j}). \tag{2.5}$$

The last term, involving the Reynolds stress $-\overline{\tilde{u}_i \tilde{u}_j}$ of the wave-induced motion, makes the equation different from the usual mean equation for turbulent flow

and gives the effect of the waves on the mean flow. Subtracting (2.5) from (2.4) gives the dynamical equations for the organized wave:

$$\frac{\partial \tilde{u}_i}{\partial t}+\bar{u}_j\frac{\partial \tilde{u}_i}{\partial x_j}+\tilde{u}_j\frac{\partial \bar{u}_i}{\partial x_j}=-\frac{\partial \tilde{p}}{\partial x_i}+\frac{1}{Re}\frac{\partial^2 \tilde{u}_i}{\partial x_j \partial x_j}+\frac{\partial}{\partial x_j}(\overline{\tilde{u}_i\tilde{u}_j}-\tilde{u}_i\tilde{u}_j)$$
$$-\frac{\partial}{\partial x_j}(\langle u_i'u_j'\rangle-\overline{u_i'u_j'}). \quad (2.6)$$

Equations (2.3*b*) and (2.6) together describe the organized wave. However, in (2.6) there appears a term

$$\tilde{r}_{ij}\equiv\langle u_i'u_j'\rangle-\overline{u_i'u_j'}, \quad (2.7)$$

which is not known. Since this term is the difference between the phase and time averages of (minus) the Reynolds stress of the background turbulence, one can look upon $-\tilde{r}_{ij}$ as the oscillation of the background Reynolds stress due to the passage of the organized disturbance. Since we as yet have no way of finding a suitable expression for $\tilde{r}_{ij}$ or of relating $\tilde{r}_{ij}$ to $\tilde{u}_i$ we have a closure problem in the equations for the disturbance.

Some insight into the behaviour of $\tilde{r}_{ij}$ can be obtained from its dynamical equation; this we develop from the dynamical equations for the turbulence component, obtained by subtracting (2.4) from (2.1*b*), which gives

$$\frac{\partial u_i'}{\partial t}+\bar{u}_j\frac{\partial u_i'}{\partial x_j}+\tilde{u}_j\frac{\partial u_i'}{\partial x_j}+u_j'\frac{\partial \bar{u}_i}{\partial x_j}+u_j'\frac{\partial \tilde{u}_i}{\partial x_j}$$
$$=-\frac{\partial p'}{\partial x_i}+\frac{1}{Re}\frac{\partial^2 u_i'}{\partial x_j\partial x_j}+\frac{\partial}{\partial x_j}(\langle u_i'u_j'\rangle-u_i'u_j'). \quad (2.8)$$

Now, on multiplying the u_i' equations by u_j', the u_j' equation by u_i', adding to obtain a dynamical equation for $u_i'u_j'$ and taking the difference between the time average and the phase average of the resulting equation, the dynamical equation for $\tilde{r}_{ij}$ is found to be

$$\frac{\bar{D}\tilde{r}_{ij}}{Dt}+\tilde{u}_k\frac{\partial \tilde{r}_{ij}}{\partial x_k}+\tilde{u}_k\frac{\partial \overline{u_i'u_j'}}{\partial x_k}+\tilde{r}_{jk}\frac{\partial \bar{u}_i}{\partial x_k}+\tilde{r}_{ik}\frac{\partial \bar{u}_j}{\partial x_k}+\overline{u_j'u_k'}\frac{\partial \tilde{u}_i}{\partial x_k}+\overline{u_i'u_k'}\frac{\partial \tilde{u}_j}{\partial x_k}$$
$$=-\tilde{r}_{jk}\frac{\partial \tilde{u}_i}{\partial x_k}+\overline{\tilde{r}_{jk}\frac{\partial \tilde{u}_i}{\partial x_k}}-\tilde{r}_{ik}\frac{\partial \tilde{u}_j}{\partial x_k}+\overline{\tilde{r}_{ik}\frac{\partial \tilde{u}_j}{\partial x_k}}+\overline{\tilde{u}_k\frac{\partial \tilde{r}_{ij}}{\partial x_k}}+\frac{\partial}{\partial x_k}(\overline{u_i'u_j'u_k'}-\langle u_i'u_j'u_k'\rangle)$$
$$-\left\langle u_j'\frac{\partial p'}{\partial x_i}\right\rangle+\overline{u_j'\frac{\partial p'}{\partial x_i}}-\left\langle u_i'\frac{\partial p'}{\partial x_j}\right\rangle+\overline{u_i'\frac{\partial p'}{\partial x_j}}$$
$$+\frac{1}{Re}\left[\frac{\partial^2 \tilde{r}_{ij}}{\partial x_k\partial x_k}-2\left\langle\frac{\partial u_i'}{\partial x_k}\frac{\partial u_j'}{\partial x_k}\right\rangle+2\overline{\frac{\partial u_i'}{\partial x_k}\frac{\partial u_j'}{\partial x_k}}\right]. \quad (2.9)$$

The closure problem is now even more serious, for (2.9) contains many new terms that are unknown. Note that at least the third, sixth and seventh terms are of the same order of magnitude as the organized motion (i.e. $O(\tilde{u}_i)$), so that even for weak organized motions one should expect oscillations in the $\tilde{r}_{ij}$ of comparable magnitude. The chief value of (2.9) is in support of the contention that the $\tilde{r}_{ij}$ should not be neglected in the solution of (2.6).

3. Energy considerations

In spite of the fact that the wave equations are not closed, considerable insight can be obtained from consideration of the energy transfer between the mean, wave-induced and fluctuating fields. In a turbulent shear flow there is continuous dissipation of turbulent kinetic energy into internal thermal energy and concomitant transfer of turbulent energy from the mean field ('production') for replenishment. There is also continuous diffusion of turbulent kinetic energy by fluctuating motions. The travelling perturbation wave will presumably distort the turbulent field and thus alter the energy budget.

The average kinetic energy per unit mass at a point is

$$\tfrac{1}{2}\overline{u_i u_i} = \tfrac{1}{2}\overline{u}_i\overline{u}_i + \tfrac{1}{2}\overline{\tilde{u}_i\tilde{u}_i} + \tfrac{1}{2}\overline{u_i' u_i'}. \tag{3.1}$$

Equations for the three components of the total kinetic energy can be obtained by multiplying the momentum equations for $\overline{u}_i$, $\tilde{u}_i$ and u_i' by $\overline{u}_i$, $\tilde{u}_i$ and u_i' respectively, phase averaging and then time averaging. One may write the result as

$$\begin{aligned}\frac{\bar{D}}{Dt}(\tfrac{1}{2}\overline{u}_i\overline{u}_i) = {} & -\frac{\partial \overline{p}\,\overline{u}_i}{\partial x_i} - (-\overline{u_i'u_j'} - \overline{\tilde{u}_i\tilde{u}_j})\frac{\partial \overline{u}_i}{\partial x_j} - \frac{\partial}{\partial x_j}[\overline{u}_i(\overline{u_i'u_j'} + \overline{\tilde{u}_i\tilde{u}_j})] \\ & + \frac{1}{Re}\frac{\partial}{\partial x_j}\left[\overline{u}_i\left(\frac{\partial \overline{u}_i}{\partial x_j} + \frac{\partial \overline{u}_j}{\partial x_i}\right)\right] - \frac{1}{2Re}\left(\frac{\partial \overline{u}_i}{\partial x_j} + \frac{\partial \overline{u}_j}{\partial x_i}\right)\left(\frac{\partial \overline{u}_i}{\partial x_j} + \frac{\partial \overline{u}_j}{\partial x_i}\right), \end{aligned} \tag{3.2a}$$

$$\begin{aligned}\frac{\bar{D}}{Dt}(\tfrac{1}{2}\overline{\tilde{u}_i\tilde{u}_i}) = {} & -\frac{\partial}{\partial x_j}[\overline{\tilde{u}_j(\tilde{p} + \tfrac{1}{2}\tilde{u}_i\tilde{u}_i)}] + (-\overline{\tilde{u}_i\tilde{u}_j})\frac{\partial \overline{u}_i}{\partial x_j} \\ & - \overline{(-\langle u_i'u_j'\rangle)\frac{\partial \tilde{u}_i}{\partial x_j}} - \frac{\partial}{\partial x_j}[\overline{\tilde{u}_i\langle u_i'u_j'\rangle}] \\ & + \frac{1}{Re}\frac{\partial}{\partial x_j}\left[\overline{\tilde{u}_i\left(\frac{\partial \tilde{u}_i}{\partial x_j} + \frac{\partial \tilde{u}_j}{\partial x_i}\right)}\right] - \frac{1}{2Re}\left(\overline{\frac{\partial \tilde{u}_i}{\partial x_j} + \frac{\partial \tilde{u}_j}{\partial x_i}}\right)\left(\overline{\frac{\partial \tilde{u}_i}{\partial x_j} + \frac{\partial \tilde{u}_j}{\partial x_i}}\right), \end{aligned} \tag{3.2b}$$

$$\begin{aligned}\frac{\bar{D}}{Dt}(\tfrac{1}{2}\overline{u_i'u_i'}) = {} & -\frac{\partial}{\partial x_j}[\overline{u_j'(p' + \tfrac{1}{2}u_i'u_i')}] + (-\overline{u_i'u_j'})\frac{\partial \overline{u}_i}{\partial x_j} \\ & + \overline{(-\langle u_i'u_j'\rangle)\frac{\partial \tilde{u}_i}{\partial x_j}} - \overline{\tilde{u}_j\frac{\partial}{\partial x_j}\langle \tfrac{1}{2}u_i'u_i'\rangle} \\ & + \frac{1}{Re}\frac{\partial}{\partial x_j}\left[\overline{u_i'\left(\frac{\partial u_i'}{\partial x_j} + \frac{\partial u_j'}{\partial x_i}\right)}\right] - \frac{1}{2Re}\left(\overline{\frac{\partial u_i'}{\partial x_j} + \frac{\partial u_j'}{\partial x_i}}\right)\left(\overline{\frac{\partial u_i'}{\partial x_j} + \frac{\partial u_j'}{\partial x_i}}\right), \end{aligned} \tag{3.2c}$$

where

$$\frac{\bar{D}}{Dt} \equiv \frac{\partial}{\partial t} + \overline{u}_j\frac{\partial}{\partial x_j}. \tag{3.2d}$$

The term on the left-hand side of each of the above equations denotes the net rate of increase of the energy component, and the terms on the right describe the mechanisms governing this change.

Let us focus our attention on the right-hand side of (3.2*b*), which describes the change in the kinetic energy of the organized wave. The first, fourth and fifth terms will vanish upon integration over a large volume of the flow, and hence represent transport of energy within the flow. The last term represents viscous dissipation of the organized motion. The second term,

$$(-\overline{\tilde{u}_i\tilde{u}_j})\,\partial \overline{u}_i/\partial x_j, \tag{3.3a}$$

represents the production of disturbance energy by action of the mean field $\overline{u}_i$ against the wave Reynolds stresses $(-\overline{\tilde{u}_i\tilde{u}_j})$. Note that this term appears as an energy drain in (3.2*a*). The third term in (3.2*b*) may be written as

$$-(\overline{-\tilde{r}_{ij}})\,\overline{\partial\tilde{u}_i/\partial x_j} \tag{3.3b}$$

and represents a drain of energy to the turbulence field by the action of the wave field $\tilde{u}_i$ against the perturbations in the background Reynolds stresses $(-\tilde{r}_{ij})$. Note that this term appears as an *input* term in (3.2*c*).

It is likely that, over most of the flow, (3.3*a*, *b*) are the two dominant terms in the energy balance for the organized motion. The wave tries to sustain itself with its own Reynolds stresses, but is broken down by the change that the wave itself produces in the background turbulence. This emphasizes the importance of $\tilde{r}_{ij}$ in governing the behaviour of the organized wave.

4. Linearized equations for parallel flows

In a linearized analysis we neglect the terms quadratic in $\tilde{u}_i$ in the momentum equations (2.6), but retain $\tilde{r}_{ij}$ because we expect it to be of importance even at first order. Consider now a parallel mean flow, statistically homogeneous in the streamwise (x_1) and spanwise (x_3) directions, i.e. $\overline{u}_i = [\overline{u}(x_2), 0, 0]$. The coefficients in the linearized equations for $\tilde{u}_i$ depend only upon x_2 and hence yield normal-mode solutions which are exponential functions of x_1, x_3 and t (Lin 1955, §1.3). One can therefore seek normal-mode disturbance (wave) solutions for each variable f of the form

$$\tilde{f} = \tfrac{1}{2}[\hat{f}(x_2)\,e^{i(\alpha x_1+\beta x_3-\omega t)} + \text{conjugate}]. \tag{4.1}$$

Here $\hat{f}$ represents the complex amplitude of the quantity $\tilde{f}$, α and β are the streamwise and spanwise wavenumbers respectively, and ω is the frequency of the oscillating disturbance. We are here interested in the cases in which β and ω are real and α is complex. Hence the wave speed c is complex. Equation (4.1) represents a wave travelling obliquely to the main flow at an angle $\tan^{-1}(\beta/\alpha_r)$ to the x_3 direction. At any point the disturbance oscillates with frequency ω. The disturbance appears as a wave travelling downstream with speed $V_c = \omega/\alpha_r$, with amplitude decaying in the streamwise direction like $\exp(-\alpha_i x)$.

On substituting (4.1) for each of the oscillating quantities in (2.3*b*) and (2.6), one obtains the following set of coupled differential equations for the perturbation wave amplitudes:

$$i\alpha\hat{u}_1 + D\hat{u}_2 + i\beta\hat{u}_3 = 0, \tag{4.2a}$$

$$(-i\omega + i\alpha\overline{u})\begin{pmatrix}\hat{u}_1\\ \hat{u}_2\\ \hat{u}_3\end{pmatrix} + D\overline{u}\begin{pmatrix}\hat{u}_2\\ 0\\ 0\end{pmatrix} = \begin{pmatrix}-i\alpha\hat{p}\\ -D\hat{p}\\ -i\beta\hat{p}\end{pmatrix} + \frac{1}{Re}(D^2-\alpha^2-\beta^2)\begin{pmatrix}\hat{u}_1\\ \hat{u}_2\\ \hat{u}_3\end{pmatrix} - \begin{pmatrix}i\alpha\hat{r}_{11}+D\hat{r}_{12}+i\beta\hat{r}_{13}\\ i\alpha\hat{r}_{21}+D\hat{r}_{22}+i\beta\hat{r}_{23}\\ i\alpha\hat{r}_{31}+D\hat{r}_{32}+i\beta\hat{r}_{33}\end{pmatrix}, \tag{4.2b,c,d}$$

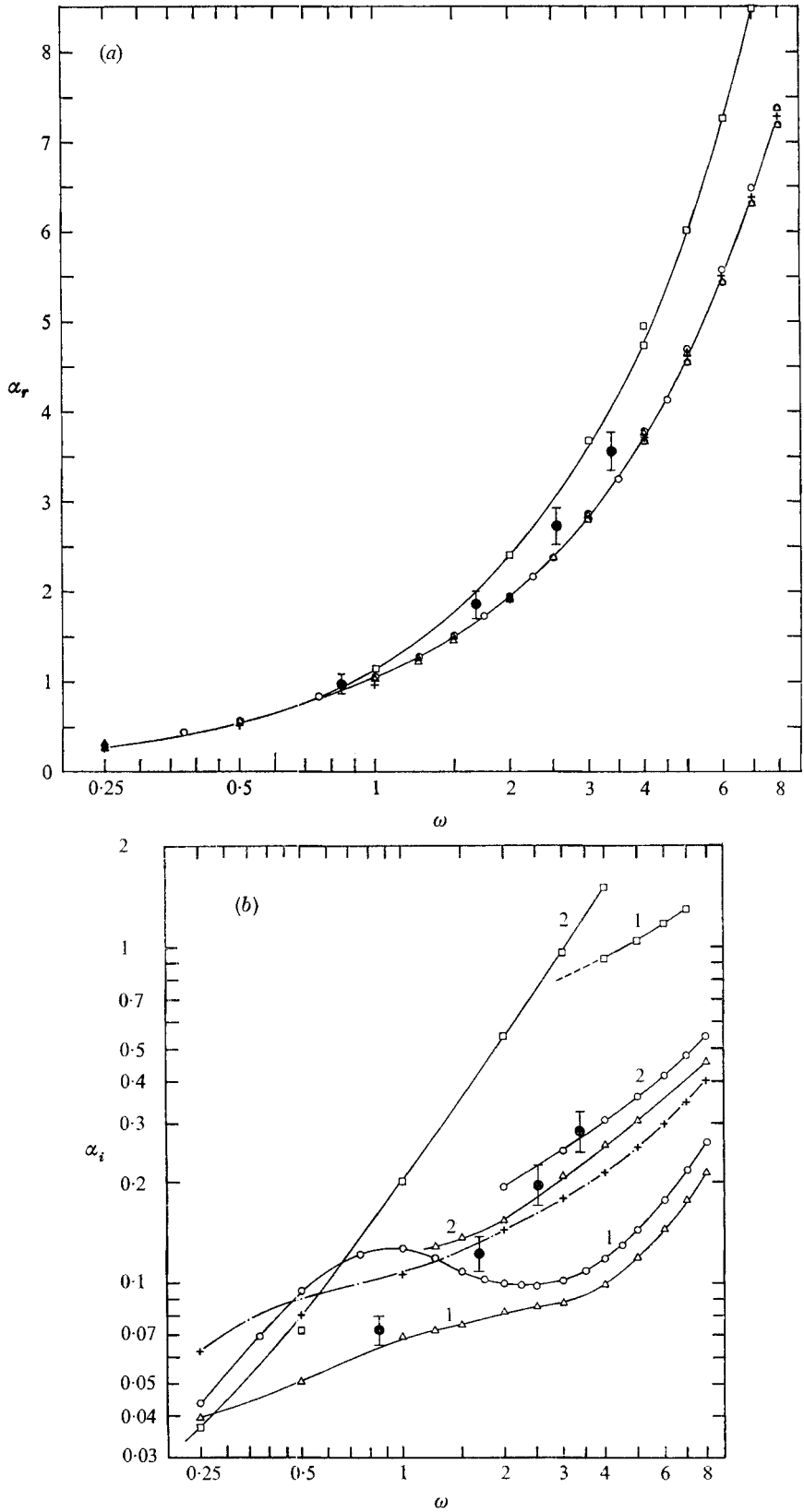

FIGURE 1. Comparison with data of (*a*) α_r and (*b*) α_i for different models. □, model (i); △, model (ii); ○, model (iii); +, model (iii), antisymmetric; ●, data.

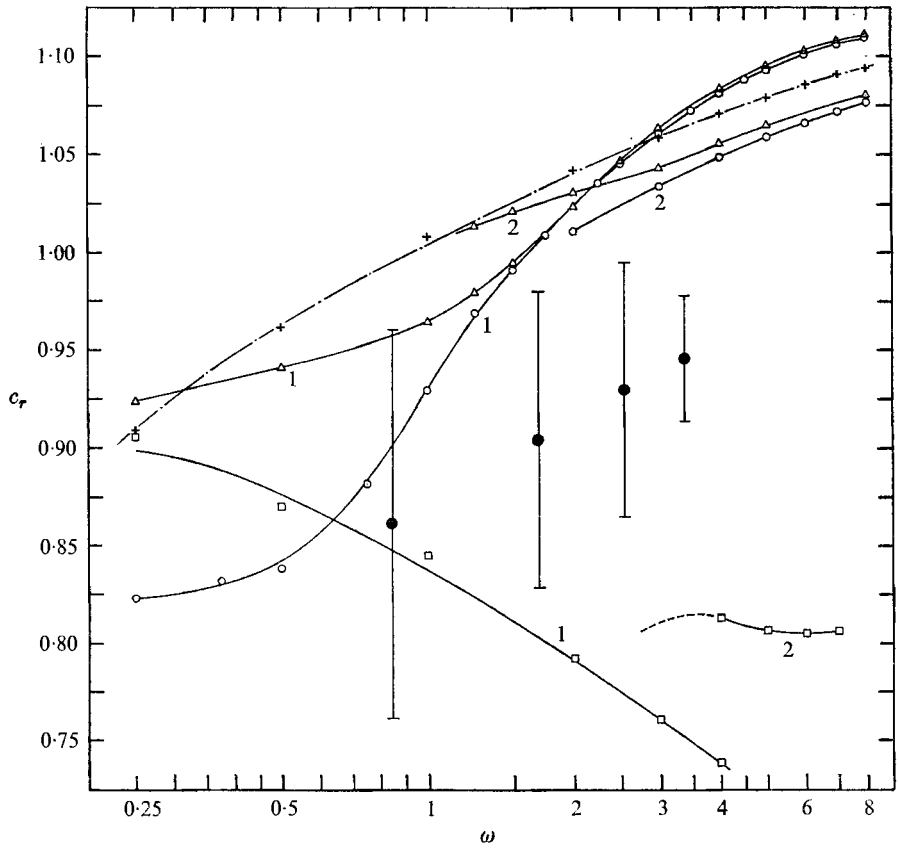

FIGURE 2. c_r for different models compared with data. Notation as in figure 1.

where $D \equiv d/dx_2$. The above equations differ from the similar equations for perturbation waves in laminar shear flow by the addition of the terms arising from oscillating Reynolds stresses. These equations do not form a closed set, for the $\hat{r}_{ij}$ terms are as yet unspecified.

A transformation in the spirit of Squire (Lin 1955, § 3.1) may be used to simplify the problem. We let

$$\left.\begin{aligned} &\alpha^2+\beta^2 = k^2, \quad \alpha\hat{u}_1+\beta\hat{u}_3 = k\hat{u}, \quad \hat{u}_2 = \hat{v}, \quad c = \omega/\alpha,\\ &\alpha\hat{r}_{12}+\beta\hat{r}_{23} = k\hat{s}_{12},\\ &\alpha^2\hat{r}_{11}+2\alpha\beta\hat{r}_{13}+\beta^2\hat{r}_{33} = k^2\hat{s}_{11}, \quad \hat{r}_{22} = \hat{s}_{22}. \end{aligned}\right\} \tag{4.3}$$

It is assumed that $\hat{r}_{ij}$ will be compatible with such a transformation. Substitution of (4.3) in (4.2) gives

$$ik\hat{u}+D\hat{v} = 0, \tag{4.4a}$$

$$i\alpha(\bar{u}-c)\hat{u}+(D\bar{u})\frac{\alpha}{k}\hat{v} = -ik\hat{p}+\frac{1}{Re}(D^2-k^2)\hat{u}-ik\hat{s}_{11}-D\hat{s}_{12}, \tag{4.4b}$$

$$i\alpha(\bar{u}-c)\hat{v} = -D\hat{p}+\frac{1}{Re}(D^2-k^2)\hat{v}-i\alpha\hat{s}_{12}-D\hat{s}_{22}. \tag{4.4c}$$

Equation (4.4*b*) results from multiplication of (4.2*b*) by α and (4.2*d*) by β, adding, and dividing by k. Note that (4.4) are of the same form as (4.2) for

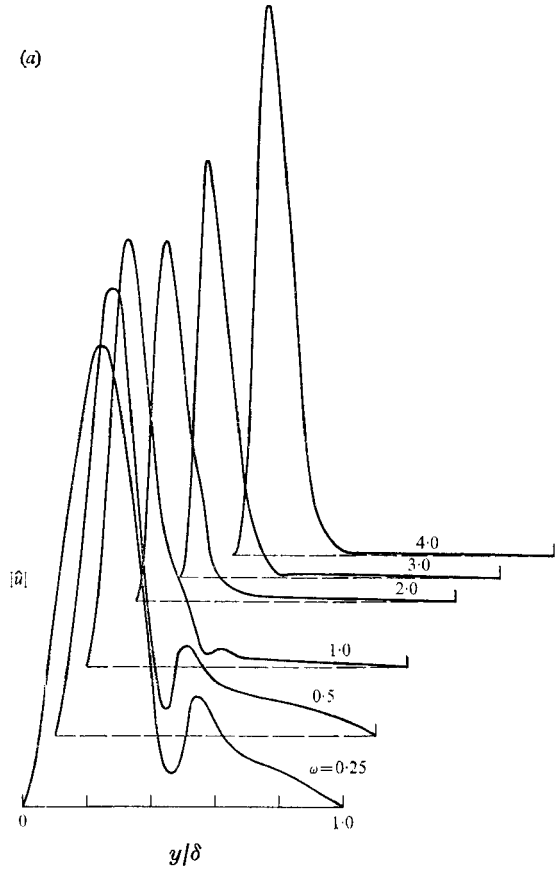

FIGURE 3. (a) $\hat{u}$ amplitudes and (b) corresponding $\hat{u}$ phase distributions at $Re_m = 12200$ for model (i).

$\beta = \hat{u}_3 = \hat{r}_{i3} = 0$. In a sense, we have reduced the oblique wave problem represented by (4.2) to an equivalent two-dimensional wave. This view of the transformation is only correct for real α, which is not the case of interest here. The transformation remains valid for complex α even though the interpretation does not.

We now substitute (4.4*a*) in (4.4*b*) and then eliminate $\hat{p}$ to obtain a single fourth-order ordinary differential equation satisfied by $\hat{v}$:

$$\alpha[(\overline{u}-c)(D^2-k^2)-D^2\overline{u}]\hat{v} = -(i/Re)(D^2-k^2)^2\hat{v} + ik^2D(\hat{s}_{11}-\hat{s}_{22})+k(D^2+k^2)\hat{s}_{12}. \quad (4.5)$$

This equation differs from the Orr–Sommerfeld equation (Lin 1955) in the addition of the oscillating Reynolds stress terms $\hat{s}_{ij}$. To solve this equation, one still needs a closure assumption for $\tilde{r}_{ij}$ to fix $\hat{s}_{ij}$. It should be mentioned that the two-dimensional problem has been developed directly by Phillips (1967, §4.3 *et seq.*) in connexion with the generation of ocean waves by wind.

The boundary conditions on the wave field are

$$\tilde{u}_i = 0 \quad \text{at solid boundaries,}$$

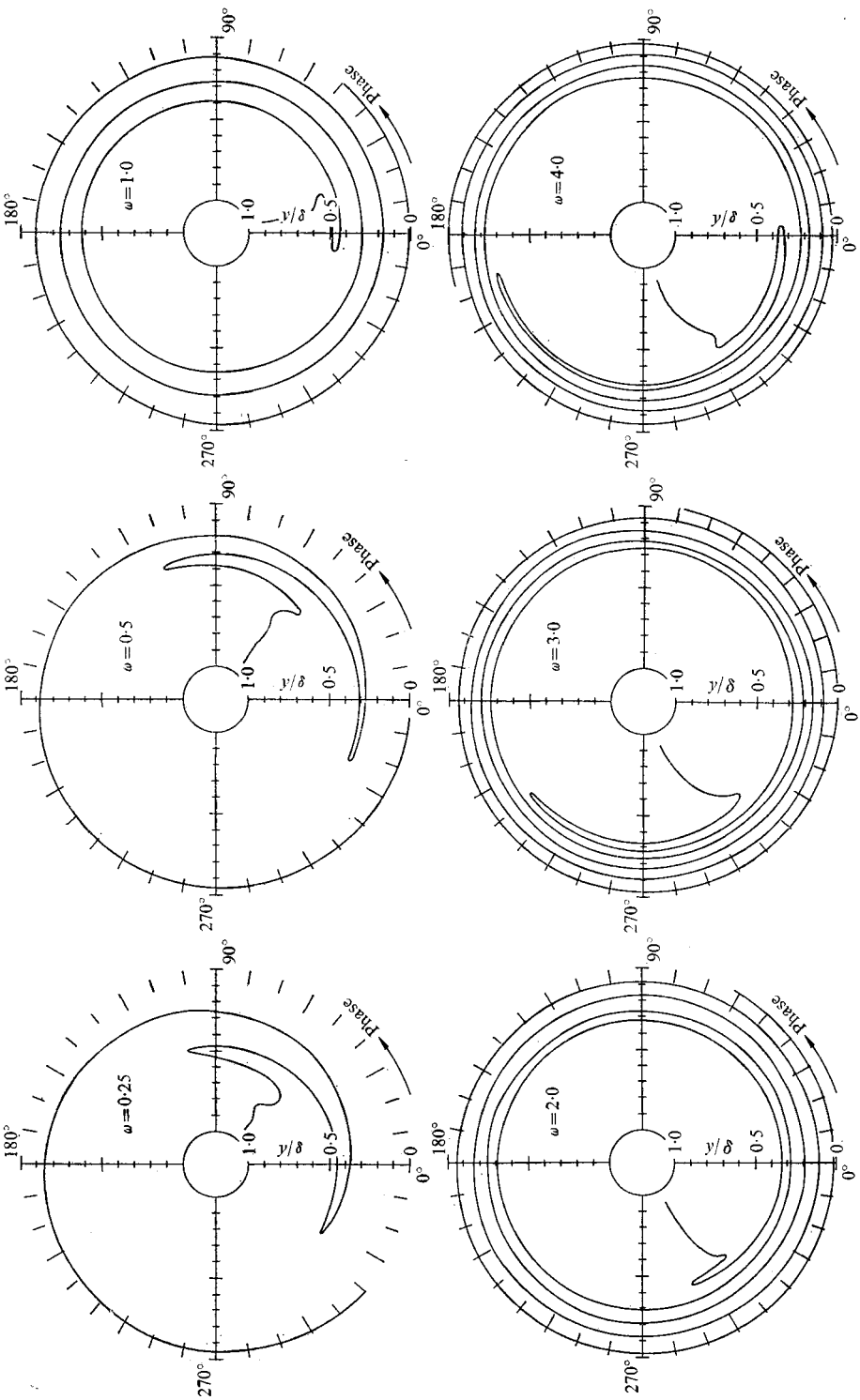

FIGURE 3 (*b*). For legend see facing page.

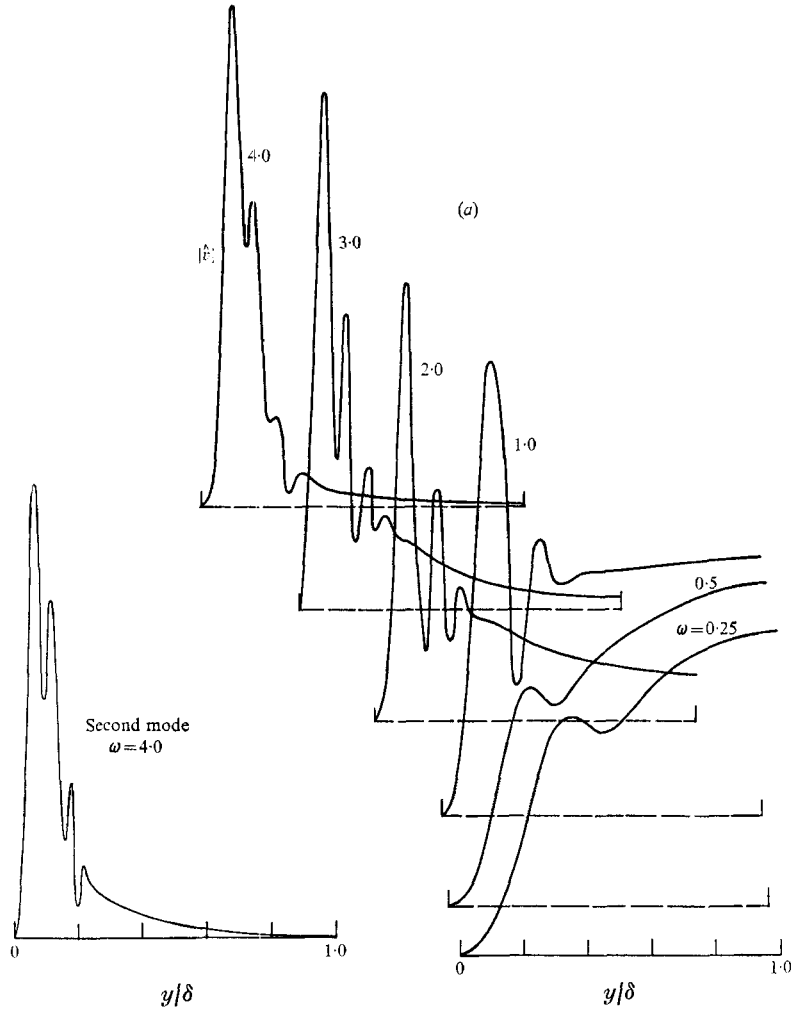

FIGURE 4. (*a*) $\hat{v}$ amplitudes and (*b*) corresponding $\hat{v}$ phase distributions at $Re_m = 12200$ for model (i).

which gives $$\tilde{v} = D\tilde{v} = 0 \quad \text{at solid boundaries.} \tag{4.6}$$

Equations (4.5) and (4.6), together with equations relating the $\hat{s}_{ij}$ to $\hat{v}$ and its derivatives, form an eigenvalue problem of the Orr–Sommerfeld type. Here we regard ω as fixed and treat α as the complex eigenvalue with $\hat{v}(y)$ as the eigenfunction. The response of the flow to a vibrating ribbon constitutes an initial-value problem for which the solution would be expressed as an expansion in terms of the eigensolutions. Hence, the eigensolutions are of primary interest.

5. Some possible closure schemes

Several possible closure schemes were investigated in connexion with this and associated work. The simplest is the *quasi-laminar model*, in which we set

$$\tilde{r}_{ij} = 0 \tag{5.1}$$

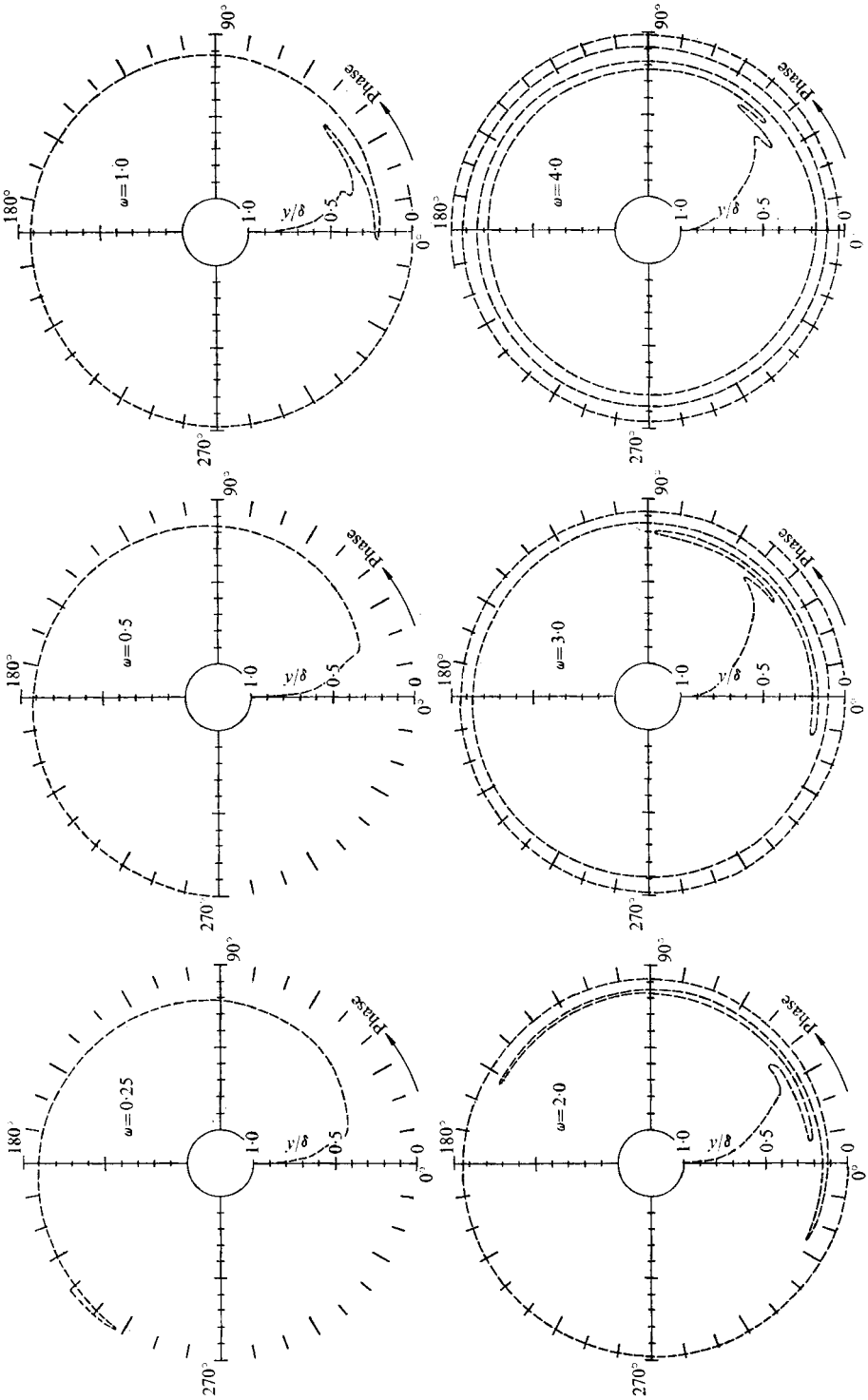

FIGURE 4(*b*). For legend see facing page.

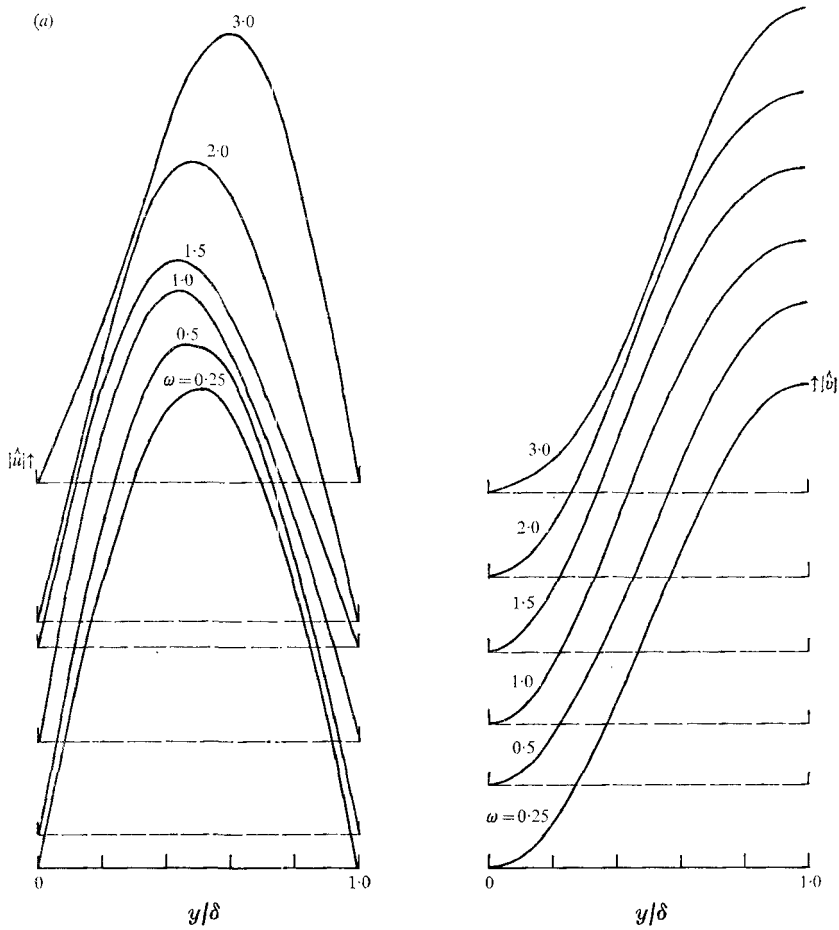

FIGURE 5. (*a*) First mode $\hat{u}$ and $\hat{v}$ amplitudes and (*b*) corresponding $\hat{u}$ (——) and $\hat{v}$ (– – –)phase distributions at $Re_m = 12200$ for model (ii).

but use the mean velocity field $\overline{u}$ appropriate to turbulent flow in the Orr–Sommerfeld solution. This is equivalent to assuming that the turbulence affects the wave only indirectly, through the mean velocity profile, and not directly, through its stresses.

A second model, which is more successful, might be termed the Newtonian eddy model. Use of this model was originally motivated by the remarkable success that it enjoys in the prediction of weakly strained turbulent shear flows, such as the far field in jets and wakes. Recently it has been given a more substantial analytical basis. The model goes back to Townsend (1956), who suggested that persistently strained turbulence should develop an equilibrium structure that depends only on the type of strain and not upon the strain-rate magnitude. This notion of an equilibrium structure has been widely accepted and given various physical interpretations. Lighthill (1956) proposed a constitutive equation for the turbulence structure, based on Townsend's data:

$$\overline{u_i' u_j'} = \tfrac{1}{3} q^2 \delta_{ij} - a q^2 S_{ij} / (S_{kl} S_{kl})^{\frac{1}{2}}, \tag{5.2}$$

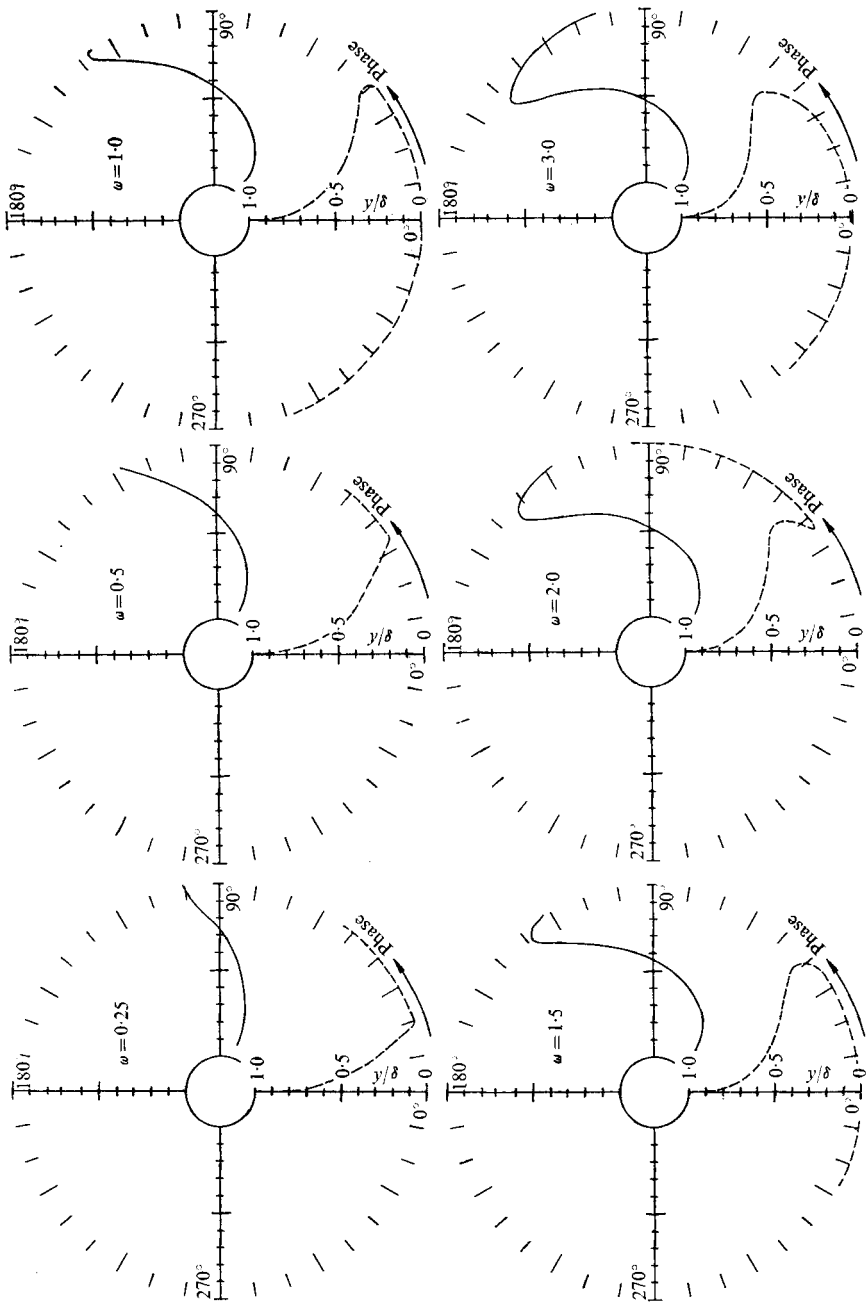

FIGURE 5(*b*). For legend see facing page.

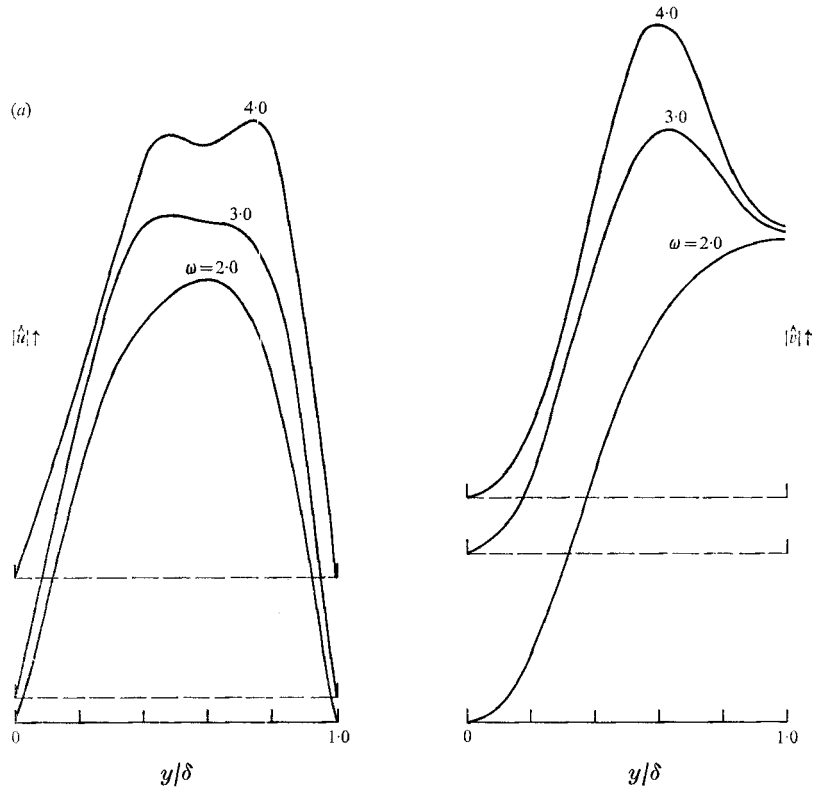

FIGURE 6. (*a*) Second mode $\hat{u}$ and $\hat{v}$ amplitudes and (*b*) corresponding $\hat{u}$ and $\hat{v}$ phase distributions at $Re_m = 12\,200$ for model (ii). Notation as in figure 5.

where
$$S_{ij} = \partial\overline{u}_i/\partial x_j + \partial\overline{u}_j/\partial x_i. \tag{5.3}$$

A somewhat different view was taken by Lumley (1967*a*), who suggested that
$$\overline{u_i' u_j'} = \tfrac{1}{3}q^2\delta_{ij} - aq^2 t^* S_{ij}, \tag{5.4}$$

where t^* is a time scale of the turbulence. The difference between (5.2) and (5.4) is critical when one proposes equations for the *disturbances* $\tilde{r}_{ij}$. Suppose we assume that the wave causes oscillation in the structure of the turbulence but not in its energy (q^2). Then, on replacing S_{ij} by $\langle S_{ij}\rangle$ and $\overline{u_i' u_j'}$ by $\langle u_i' u_j'\rangle$, (5.2) gives
$$\tilde{r}_{ij} = \frac{-aq^2}{(\overline{S}_{kl}\overline{S}_{kl})^{\frac{1}{2}}}\tilde{S}_{ij} + \frac{aq^2\overline{S}_{ij}}{(\overline{S}_{kl}\overline{S}_{kl})^{\frac{3}{2}}}\overline{S}_{mn}\tilde{S}_{mn}. \tag{5.5}$$

Now, in a parallel shear flow, where
$$\overline{\mathbf{S}} = \begin{pmatrix} 0 & \frac{1}{2}D\overline{u} & 0 \\ \frac{1}{2}D\overline{u} & 0 & 0 \\ 0 & 0 & 0 \end{pmatrix},$$

(5.5) gives
$$\tilde{\mathbf{r}} = -\frac{aq^2\sqrt{2}}{D\overline{u}}\begin{pmatrix} \tilde{S}_{11} & 0 & \tilde{S}_{13} \\ 0 & \tilde{S}_{22} & \tilde{S}_{23} \\ \tilde{S}_{13} & \tilde{S}_{23} & \tilde{S}_{33} \end{pmatrix}. \tag{5.6}$$

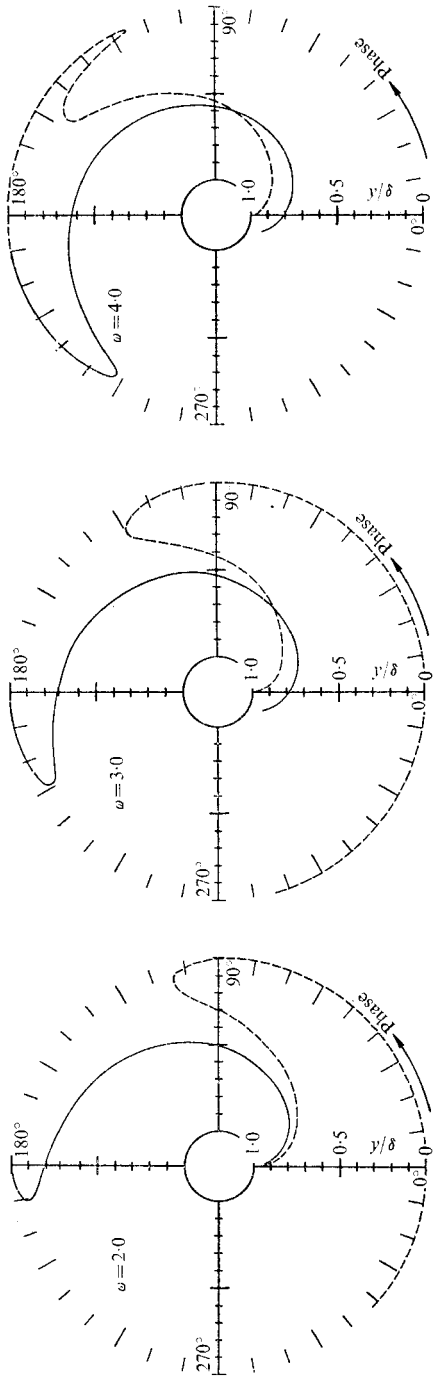

FIGURE 6 (*b*). For legend see facing page.

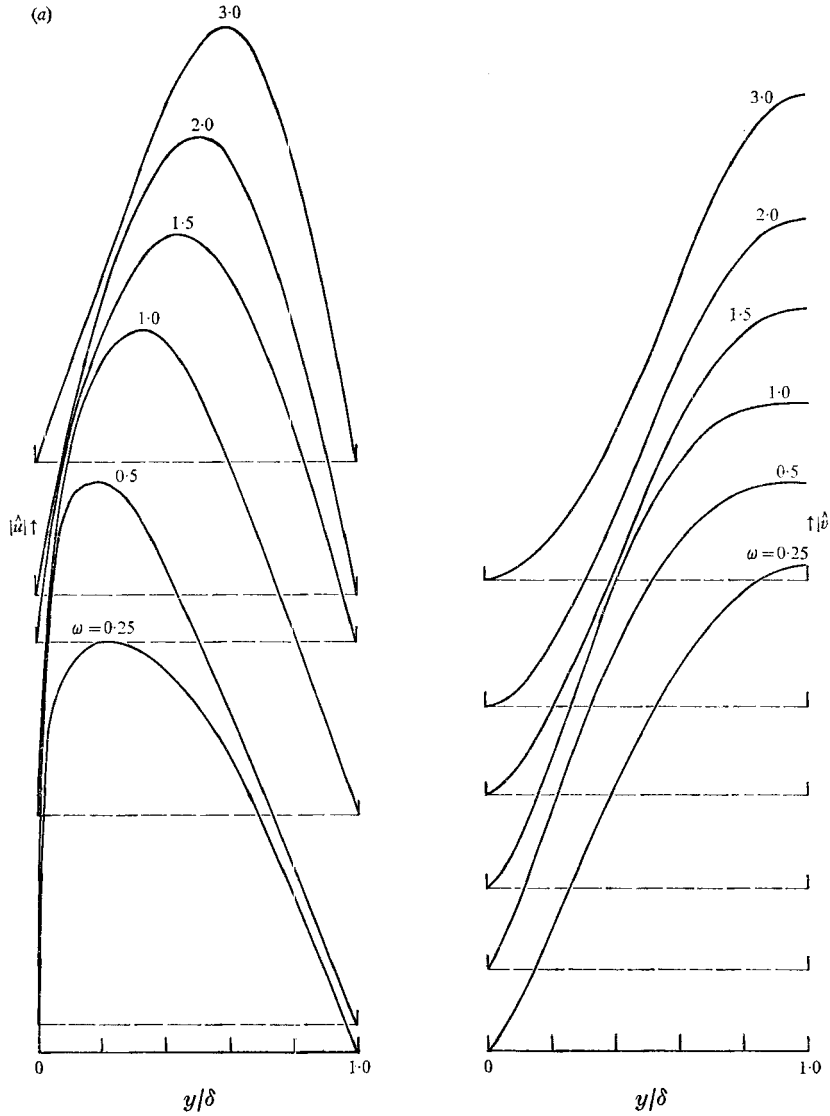

FIGURE 7. (*a*) First mode $\hat{u}$ and $\hat{v}$ amplitudes and (*b*) corresponding $\hat{u}$ and $\hat{v}$ phase distributions at $Re_m = 12200$ for model (iii). Notation as in figure 5.

Note that this model predicts *no* oscillation in the primary shearing stress, i.e. $\tilde{r}_{12} = 0$. This does not seem very reasonable; moreover, (5.6) does not pass through the Squire transformation (4.3), and hence is rather inconvenient. On the other hand if we use (5.4) and argue that neither the turbulence energy nor time scale is oscillated by the wave, we instead obtain

$$\tilde{r}_{ij} = -aq^2t^*\tilde{S}_{ij}, \tag{5.7}$$

which seems more reasonable and does conform to the Squire transformation.

Further basis for (5.7) is provided by Lumley's (1967*b*) development† of the

† Slightly modified in a footnote on page 416 of Lumley (1971).

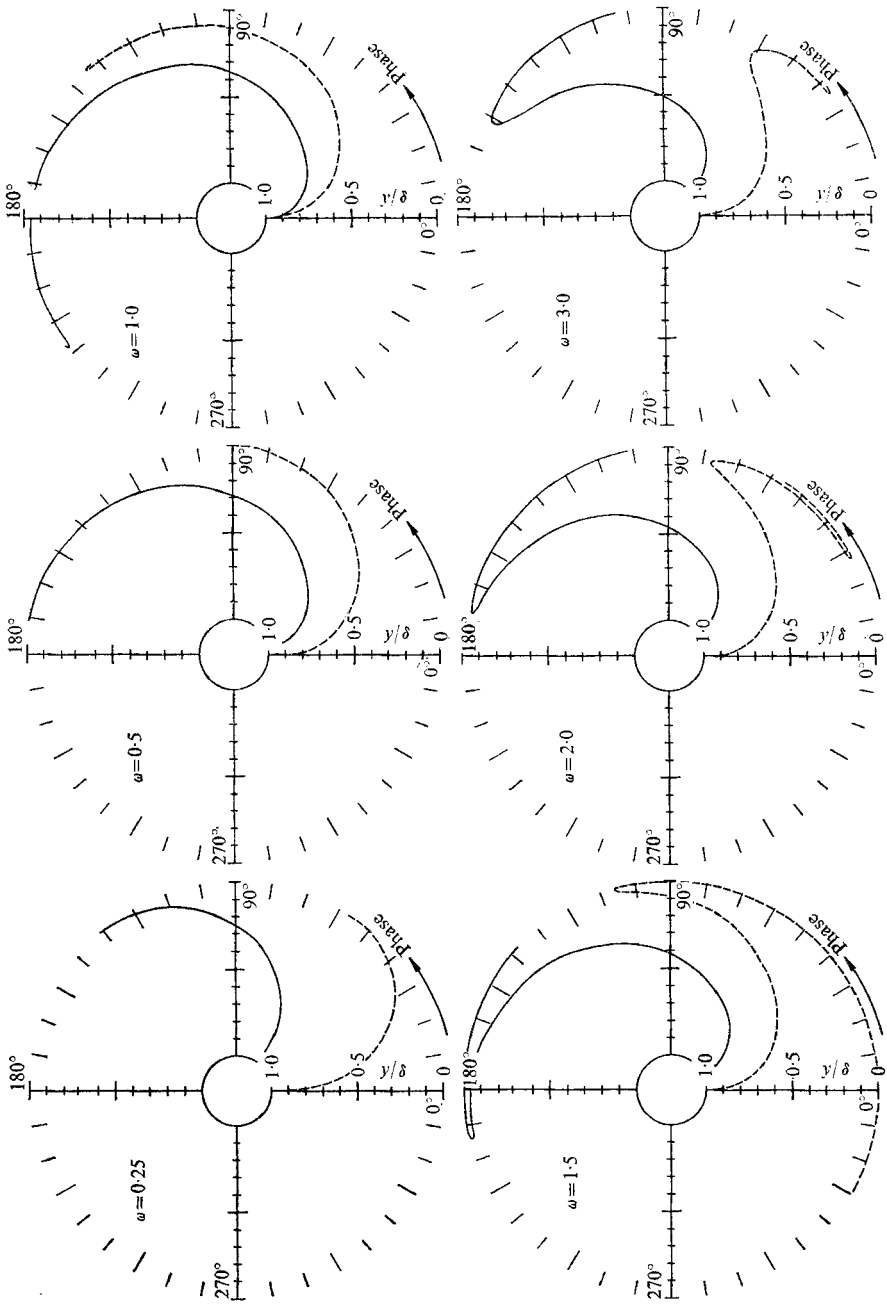

FIGURE 7 (*b*). For legend see facing page.

general functional form of the Reynolds stress deformation behaviour for a turbulence field with fading memory and limited awareness. By carrying out an expansion in terms of a memory parameter and spatial-awareness parameter, he showed that the first departure from isotropy is due to the inhomogeneity in the strain rate and that

$$\overline{u_i' u_j'} = \tfrac{1}{3}q^2\delta_{ij} - 2\epsilon S_{ij} + \text{second-order term in awareness and memory parameters.}$$

Presumably, if the strain-rate inhomogeneity is of sufficient scale and its rate of change is sufficiently slow, (5.7) will be a good approximation. Hence ϵ is a parameter of the turbulence, which Lumley identifies as

$$\epsilon = \lim_{S_{ij}\to 0} \tfrac{1}{2}(\overline{u_i' u_j'} S_{ij} / S_{kl} S_{kl}). \tag{5.8}$$

Expanding (5.8), again assuming that q^2 is not caused to oscillate by the wave, we have

$$\tilde{r}_{ij} = -2\epsilon \tilde{S}_{ij}, \tag{5.9}$$

which is of course equivalent to (5.7). Equation (5.9) is called the *Newtonian eddy model*; it is equivalent to a constitutive equation relating the Reynolds stress oscillations to the oscillating strain rate through a scalar eddy viscosity. In view of the discussion, we might expect (5.9) to work best for relatively low frequency weak oscillations, having a wavelength considerably larger than the dominant scales of turbulence. The experiments reported in II are of this nature. The notion of an equilibrium structure that underlies (5.4) has recently been demolished by Lumley (1971), who showed that persistently strained homogeneous turbulence will never attain an equilibrium structure. Clearly, (5.9) must be regarded as a model to be tested rather than something physical, and we shall study it in this spirit.

Some thought and analysis has been devoted to more complicated closure models. One possibility is to use (2.9) as a basis, neglecting all the terms that cannot be represented in terms of $\tilde{u}_1$ and $\tilde{r}_{ij}$, and neglecting nonlinear terms. Then, upon introduction of the wave decomposition for parallel flows, one obtains

$$i\alpha(\bar{u}-c)\hat{r}_{ij} + \hat{u}_2 D\bar{r}_{12} + \hat{r}_{j2} D\bar{u}\delta_{i1} + \hat{r}_{i2} D\bar{u}\delta_{j1} + \bar{r}_{jk}\begin{pmatrix} i\alpha\delta_{k_1} \\ D\delta_{k_2} \\ i\beta\delta_{k_3} \end{pmatrix}\hat{u}_i + \bar{r}_{ik}\begin{pmatrix} i\alpha\delta_{k_1} \\ D\delta_{k_2} \\ i\beta\delta_{k_3} \end{pmatrix}\hat{u}_j = \frac{1}{Re}(D^2 - k^2)\hat{r}_{ij}, \tag{5.10}$$

where $\bar{r}_{ij} = \overline{u_i' u_j'}$. Equation (5.10) can be carried through the Squire transformation and then, in conjunction with (4.5), yields a tenth-order system. Asymptotic analysis of this system indicates extremely rapidly growing solutions away from the critical layer (the point where $\bar{u} = c$). In addition, if the viscous terms are neglected (5.10) is singular at the critical layer and this singularity is *stronger* than in conventional Orr–Sommerfeld problems. Some numerical calculations based on (5.10) were actually carried out using a two-level filtering technique (Lee &

Reynolds 1967) and special integrating algorithms. Crow (private communication) correctly criticized this approach on the grounds that the pressure–velocity term contains a first-order term that is probably of considerable importance but is not included in (5.9); further exploration of this model was then abandoned. It would be interesting to try one of the better turbulence model equation systems currently being developed for steady turbulent flows (Reynolds 1972), but as yet this has not been attempted.

6. The wave equation

On using (5.9), (4.5) becomes

$$\alpha[(\overline{u}-c)(D^2-k^2)-D^2\overline{u}]\,\hat{v} = -(i/R)(D^2-k^2)^2\hat{v} - i\bar{E}(D^2-k^2)^2\hat{v} - 2i(D\bar{E})(D^3-k^2D)\hat{v} - i(D^2\bar{E})(D^2+k^2)\hat{v}. \quad (6.1)$$

Here $\bar{E}$ is the local eddy viscosity of the basic flow, normalized using the reference length and velocity: $\bar{E} = \epsilon/(U_r\delta) = 1/R_\epsilon$,

where R_ϵ is a reciprocal Reynolds number based on eddy viscosity. Equation (6.1) is precisely the Orr–Sommerfeld equation for a fluid with a prescribed local viscosity (Betchov & Criminale 1967). In typical turbulent shear flows R_ϵ is of the order of 10–100, while R is much larger, hence the turbulence terms will certainly be very important. In ordinary viscous flows the effects of viscosity are concentrated near the wall and near the critical layer in regions of the order of $(\alpha R)^{-\frac{1}{3}}\delta$ in thickness. At high Reynolds numbers these layers are very thin, and this has served as the basis for various approximate treatments. The effect of the turbulence terms will be of order $(\alpha R_\epsilon)^{-\frac{1}{3}}\delta$, which in many problems will constitute a significant portion of the total flow field. These considerations indicate that the 'inviscid' theories are not likely to be reasonable models for organized waves in turbulent shear flows.

The mean velocity profile $\overline{u}$ and the corresponding eddy viscosity ϵ must be specified before (6.1) can be solved. Our experiments dealt with two-dimensional channel flow, for which we have previously used a convenient expression for the eddy viscosity (Reynolds & Tiederman 1967):

$$E = \frac{\epsilon}{\nu} = \frac{1}{2}\left\{1+\kappa^2\frac{Re_m^2B^2}{9}[2y-y^2]^2[3-4y+y^2]^2\left[1-\exp\left(\frac{-yRe_m\sqrt{B}}{A^+}\right)\right]^2\right\}^{\frac{1}{2}} - \tfrac{1}{2}. \quad (6.2)$$

Here Re_m is $U_m\delta/\epsilon$, where U_m is the average velocity in the channel (continuity average) and δ is the channel half-width, and y is the distance from the wall (x_2), normalized with δ. Our experiments (I, II) correspond to $Re_m = 12\,200$, for which all of our calculations were made. The parameters A^+ and κ may be freely varied. A^+ is the constant in Van Driest's wall law characterizing the thickness of the wall-layer flow co-ordinates, and κ is the von Kármán constant. $B \equiv -dP_w/dx$ (normalized) must be calculated. The momentum equation is (normalized using U_m and δ)

$$-B = \frac{dP_w}{dx} = \frac{1}{Re_m}\frac{d}{dy}\left[(1+E)\frac{d\overline{u}}{dy}\right]. \quad (6.3)$$

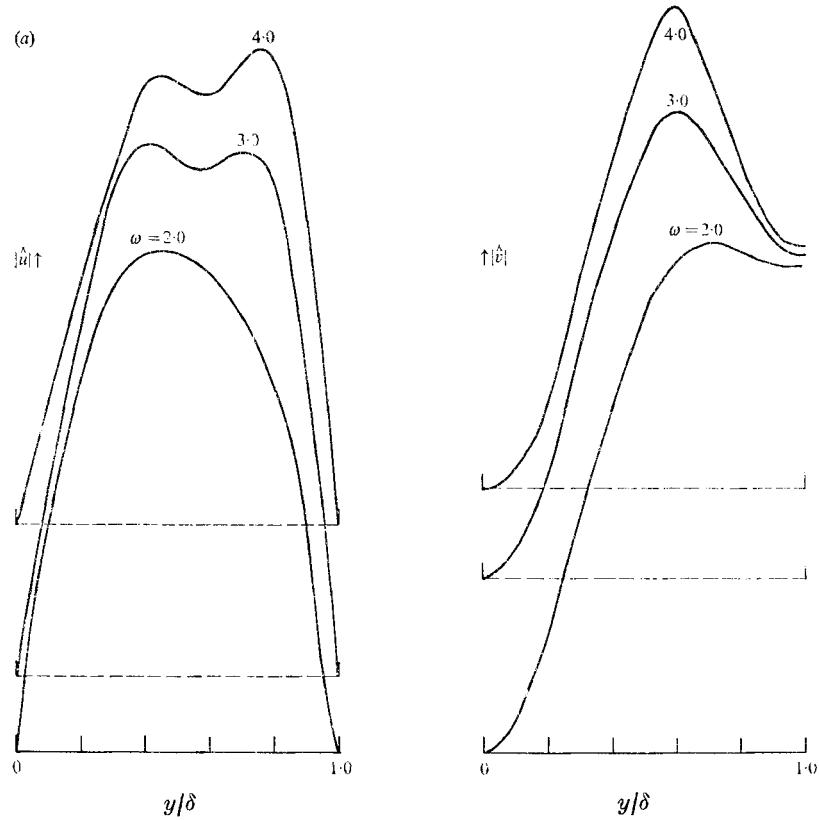

FIGURE 8. (*a*) Second mode $\hat{u}$ and $\hat{v}$ amplitudes and (*b*) corresponding $\hat{u}$ and $\hat{v}$ phase distributions at $Re_m = 12200$ for model (iii). Notation as in figure 5.

Integrating twice yields

$$\overline{u}(y) = Re_m B \int_0^y \frac{1-y_1}{1+E(y_1)}\, dy_1. \tag{6.4}$$

For given Re_m, A^+ and κ, (6.3) fixes E, and (6.4) gives $\overline{u}$ for a trial value of B. B must then be adjusted to give the proper mean velocity, i.e. until

$$1 = \int_0^1 \overline{u}(y)\, dy. \tag{6.5}$$

The B iteration is rapidly convergent. Once B is known, $\overline{u}$, ϵ and their derivatives can be readily calculated. A number of trial calculations were made with different values of A^+ and κ and the calculated $\overline{u}(y)$ were compared with the measured profile (see I). The best fit was obtained with $A^+ = 29$ and $\kappa = 0{\cdot}45$, and these values were used in the calculations. For comparisons with our experiment see R.

In the calculations outlined above, and in the solution of (6.1), a variable y mesh was used. The mesh consisted of eight parts, each having 50 points, with the spacing doubling between adjacent parts. Values of $\overline{u}$, $\overline{E}$ and their derivatives were precomputed at each mesh point for use in the solution of (6.1). The solution of (6.1) could employ smaller mesh steps if necessary, interpolating to obtain $\overline{u}$ and $\overline{E}$ at intermediate points.

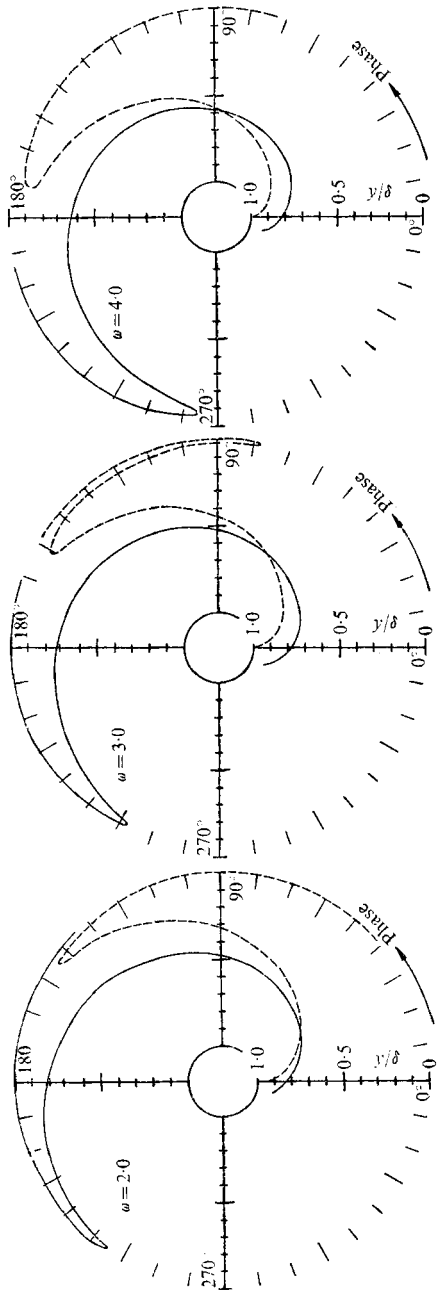

FIGURE 8 (*b*). For legend see facing page.

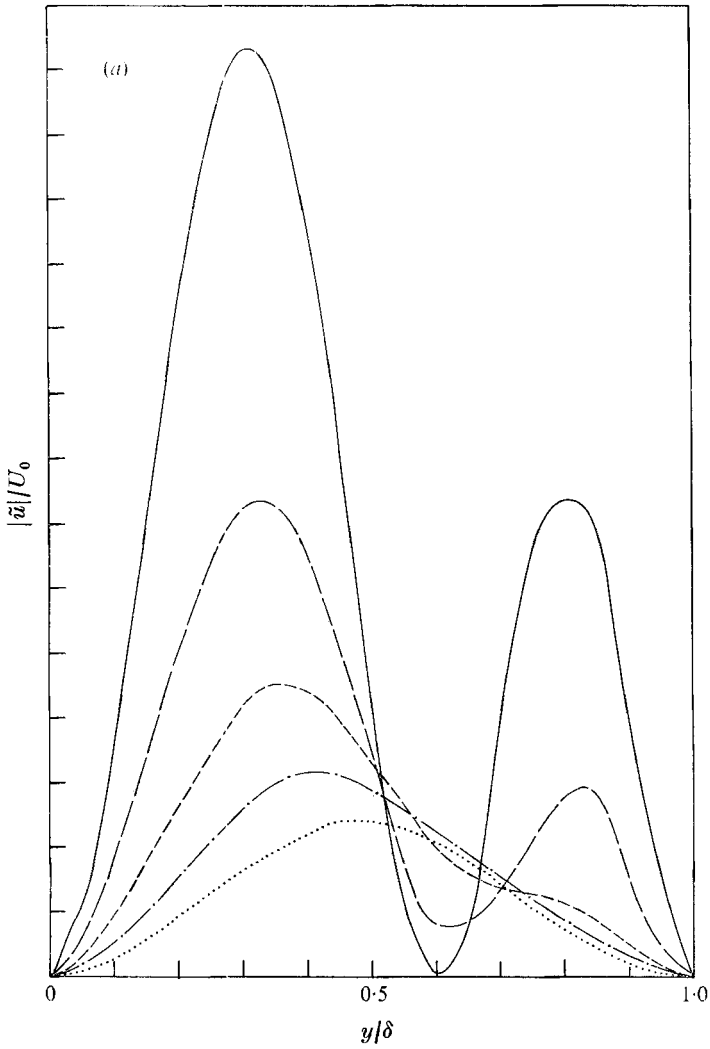

FIGURE 9. (*a*) $\hat{u}$ amplitudes and (*b*) phase distributions for the two-mode superposition. $\omega = 3{\cdot}0$, $Re_m = 12200$; —, $x/\delta = 4$; — —, $x/\delta = 6$, - - - - - -, $x/\delta = 8$; —·—, $x/\delta = 10$; · · · · · ·, $x/\delta = 12$.

The solution of (6.1) was carried out over half the channel, using either symmetric or antisymmetric boundary conditions (for $\hat{v}$) at the channel centre-line. Experience with laminar flow suggested that the symmetric eigenfunctions would be most interesting, so both the experiments (II) and calculations concentrated on symmetric eigensolutions. Starting with a trial value for the eigenvalue α, two linearly independent solutions to (6.1), each satisfying the centre-line boundary conditions, were constructed by numerical integration towards the wall. The Kaplan filtering technique (Lee & Reynolds 1967) was used to maintain linear independence. Once the wall had been reached, a properly normalized linear combination of the two solutions that satisfied one of the wall boundary conditions was formed. Then, the calculation was repeated with adjusted values of

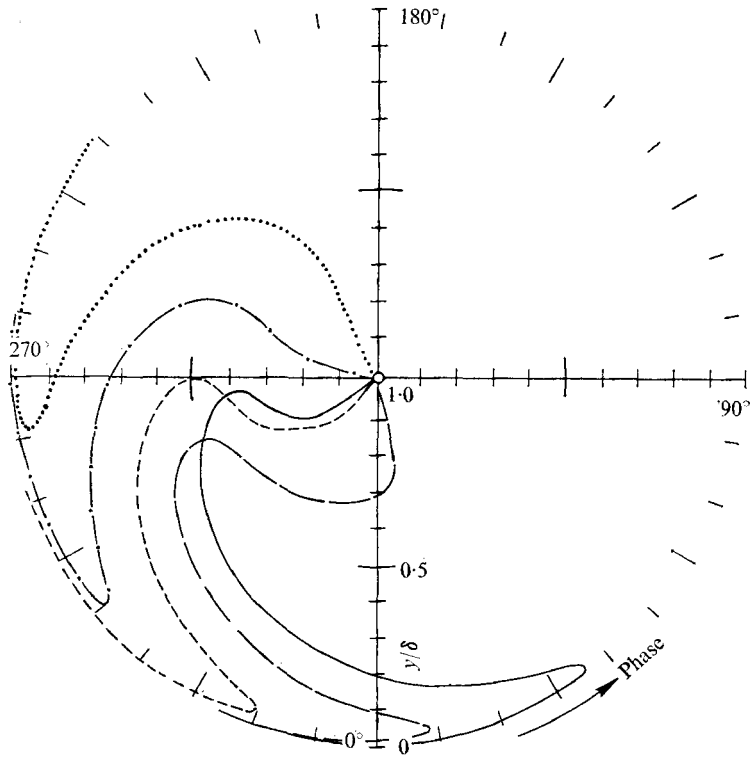

FIGURE 9(*b*). For legend see facing page.

the eigenvalue α until the second wall boundary condition was also satisfied. The eigenfunctions were normalized to make the value of $\hat{v}$ at the centre-line equal unity (or the value of $D\hat{v}$ unity for antisymmetric disturbances). With $\hat{v}$ known, the streamwise component $\hat{u}$ was calculated from (4.4*a*). All calculations were done in FORTRAN using the automatic complex arithmetic provisions. The program used was a simple adaptation of ORRSOM (Reynolds 1969) and is given in R.

7. Computational results and comparisons with experiments

Detailed calculations were made for the following three models. (i) Quasi-laminar ($E = 0$). (ii) Constant $\bar{E}(\approx \frac{1}{300})$, corresponding to $E = \epsilon/\nu = 40$. (iii) Variable $\bar{E}(= E(y))$ calculated using (6.2). For all calculations $\beta = 0$ so $\alpha = k$, to correspond with the two-dimensional waves studied in the experiments. In these calculations, and in the comparisons with the data, the parameters were normalized using the average velocity U_m and the channel half-width δ. For this flow, U_0, the centre-line velocity used in the normalizations in II, was $1{\cdot}14U_m$. Figure 1 shows the calculated eigenvalue α as a function of the (dimensionless) frequency. For given frequency ω, there are presumably an infinite number of eigensolutions having different eigenvalues. We chose to rank the eigenfunctions according to the value of α_i; the 'least-damped' mode (with smallest α_i) is designated the first

mode, etc. For most frequencies the eigenvalue search yielded two modes, designated by 1 and 2 in figure 1 (*b*). Note that the values of α_r for the two modes were nearly identical (figure 1 (*a*)).

The wavenumbers for particular frequencies, as predicted by the three models, are quite similar (see figure 1 (*a*)). Note that there is very little difference between models (ii) and (iii), and that these models predict wavenumbers slightly lower than those predicted by the quasi-laminar model. The measured wavenumbers lie slightly above those predicted by models (ii) and (iii), and about the same amount below the quasi-laminar predictions. Looking only at wavenumbers, one would not be able to select which of the models is best.

The predicted attenuation factors α_i are shown in figure 1 (*b*). Considerable differences between the various models are evident here. The data suggest that the quasi-laminar model seriously overpredicts α_i, by as much as a factor of three. The models that include some turbulence effects seem to do better, but neither is really very satisfactory.

The predicted and measured values of c_r, which for small α_i/α_r are approximately equal to the wave speed V_c (see II), are shown in figure 2. Note that the quasi-laminar model predicts a decrease in c_r with increased frequency, while the turbulent models and the data show an increase in c_r with increasing frequency. This comparison again suggests that the quasi-laminar model is not very adequate; however, the turbulent models predict speeds that are somewhat too high, suggesting there is considerable room for improvement in the theory.

The amplitude and phase of the $\tilde{u}$ component of the eigenfunctions are shown for several frequencies in figures 3–8. Figures 3 and 4 show the quasi-laminar eigenfunctions, which are strongly peaked near the wall and exhibit rapid phase oscillations particularly at the higher frequencies. These predictions should be compared with the corresponding experimental amplitudes and phases shown in II. In particular, the phase oscillations exhibited by the quasi-laminar model are not evident in the data, and the amplitude distribution of the quasi-laminar model seems to be too strongly peaked. This comparison is perhaps the strongest evidence supporting rejection of the quasi-laminar model.

The nature of the eigenfunctions for the simple turbulent model (ii) shown in figures 5 and 6 bears a much closer resemblance to the experiments. Note that the amplitude distributions are much flatter and the phase distributions do not have the wild oscillations exhibited by the quasi-laminar model. The more complicated eddy-viscosity distribution does not produce any qualitative difference; the predictions of model (iii) (see figures 7 and 8) are seen to be quite similar to those of model (ii) (see figures 5 and 6).

It must be remembered that the predictions so far deal with single modes. For a single mode, the shape of the amplitude and phase curves should be unchanged in the streamwise direction. The data (II) show significant changes in both, particularly close behind the vibrating ribbon. This suggests that the ribbon excites a superposition of at least two modes, which attenuate at their own rates in the streamwise direction. In order to look at this problem theoretically, we made a superposition of the first and second modes from model (ii) at $\omega = 3$, which corresponds to something between the 75 and 100 Hz data given in II. At both

frequencies the data show a strong dip and phase reversal at a point near the wall, and the dip gradually is 'filled in' at the stations downstream. Given two modes, one can of course combine them to place a zero amplitude point anywhere in the flow, and we computed the result of such a combination that has the two peaks of about the right initial amplitude on either side of the initial dip. The results are shown in figure 9. Note that this two-mode combination indeed exhibits the qualitative features of the measured data. The amplitude and phase curves are not self-similar, but become more so further downstream (where the second mode decays more rapidly that the first). The dip is gradually 'filled in', and the peaky structure gradually disappears. This calculation provides strong support for the notion that the ribbons excite multiple wavenumbers at a given frequency and that the properties of the fundamental pure mode must be estimated from the data recorded far downstream of the vibrating ribbon.

8. Conclusion

The comparisons between our experiments and model calculations indicate rather conclusively that the quasi-laminar model, in which the influence of the organized wave on the background turbulence is neglected, does not adequately describe the behaviour of waves in turbulent shear flow. It seems absolutely essential to include a term representing the wave-induced oscillations into the background turbulent stresses. A simple model that seems to possess many of the proper qualitative features is the Newtonian eddy model, and the use of a constant eddy viscosity in this model gives results that are not substantially different from those obtained with the 'actual' variable eddy viscosity. None of the models investigated to date are quantitatively very adequate, and there is need for a better model. The development of a more satisfactory model would be facilitated by direct measurements of the $\tilde{r}_{ij}$; such measurements are presently being obtained at Stanford.

This work is supported by the National Science Foundation and by the Mechanics Branch of the Air Force Office of Scientific Research. Their assistance is gratefully acknowledged.

REFERENCES

BETCHOV, R. & CRIMINALE, W. O. 1967 *Stability of Parallel Flows*. Academic.

HUSSAIN, A. K. M. F. & REYNOLDS, W. C. 1970*a* *J. Fluid Mech.* **41**, 241.

HUSSAIN, A. K. M. F. & REYNOLDS, W. C. 1970*b* The mechanics of a perturbation wave in turbulent shear flow. *Department of Mech. Eng. Rep., Stanford University*, FM-6.

HUSSAIN, A. K. M. F. & REYNOLDS, W. C. 1972 *J. Fluid Mech.* **54**, 241.

LANDAHL, M. T. 1967 *J. Fluid Mech.* **29**, 441.

LEE, L. H. & REYNOLDS, W. C. 1967 *Quart. J. Mech. Appl. Math.* **20**, 1.

LIGHTHILL, M. J. 1956 *J. Fluid Mech.* **1**, 554.

LIN, C. C. 1955 *The Theory of Hydrodynamic Stability*. Cambridge University Press.

LUMLEY, J. 1967*a* The applicability of turbulence research to the solution of the internal flow problems. In *Fluid Mechanics of Internal Flow* (ed. G. Sovran), p. 152. Elsevier.

LUMLEY, J. 1967*b* *Phys. Fluids*, **10**, 1405.

LUMLEY, J. 1971 *J. Fluid Mech.* **41**, 413.

PHILLIPS, O. M. 1967 *The Dynamics of the Upper Ocean.* Cambridge University Press.

REYNOLDS, W. C. 1969 ORRSOM: a Fortran IV program for solution of the Orr–Sommerfeld equation. *Department of Mech. Eng. Tech. Rep., Stanford University*, FM-4.

REYNOLDS, W. C. 1972 Recent advances in the computation of turbulent flows. *Advances in Chem. Engng*, to appear.

REYNOLDS, W. C. & TIEDERMAN, W. G. 1967 *J. Fluid Mech.* **27**, 465.

TOWNSEND, A. 1956 *The Structure of Turbulent Shear Flow.* Cambridge University Press.